



**HAL**  
open science

## Break of slope in earthquake size distribution and creep rate along the San Andreas Fault system

Inessa Vorobieva, Peter Shebalin, Clément Narteau

► **To cite this version:**

Inessa Vorobieva, Peter Shebalin, Clément Narteau. Break of slope in earthquake size distribution and creep rate along the San Andreas Fault system. *Geophysical Research Letters*, 2016, 43, pp.6869-6875. 10.1002/2016GL069636 . insu-03581314

**HAL Id: insu-03581314**

**<https://insu.hal.science/insu-03581314>**

Submitted on 19 Feb 2022

**HAL** is a multi-disciplinary open access archive for the deposit and dissemination of scientific research documents, whether they are published or not. The documents may come from teaching and research institutions in France or abroad, or from public or private research centers.

L'archive ouverte pluridisciplinaire **HAL**, est destinée au dépôt et à la diffusion de documents scientifiques de niveau recherche, publiés ou non, émanant des établissements d'enseignement et de recherche français ou étrangers, des laboratoires publics ou privés.

Copyright

RESEARCH LETTER

10.1002/2016GL069636

Key Points:

- Earthquake size distribution depends on the rate of aseismic deformation
- Creep is responsible for a break of slope in the earthquake size distribution
- Faster creep causes a deficit of larger earthquakes

Supporting Information:

- Supporting Information S1

Correspondence to:

I. Vorobieva,  
vorobiev@mitp.ru

Citation:

Vorobieva, I., P. Shebalin, and C. Narteau (2016), Break of slope in earthquake size distribution and creep rate along the San Andreas Fault system, *Geophys. Res. Lett.*, *43*, 6869–6875, doi:10.1002/2016GL069636.

Received 23 FEB 2016

Accepted 15 JUN 2016

Accepted article online 20 JUN 2016

Published online 8 JUL 2016

## Break of slope in earthquake size distribution and creep rate along the San Andreas Fault system

Inessa Vorobieva<sup>1,2</sup>, Peter Shebalin<sup>1,2</sup>, and Clément Narteau<sup>2</sup>

<sup>1</sup>Institute of Earthquake Prediction Theory and Mathematical Geophysics, Moscow, Russia, <sup>2</sup>Équipe de Dynamique des Fluides Géologiques, Institut de Physique du Globe de Paris, Sorbonne Paris Cité, Paris Diderot University, Paris, France

**Abstract** Crustal faults accommodate slip either by a succession of earthquakes or continuous slip, and in most instances, both these seismic and aseismic processes coexist. Recorded seismicity and geodetic measurements are therefore two complementary data sets that together document ongoing deformation along active tectonic structures. Here we study the influence of stable sliding on earthquake statistics. We show that creep along the San Andreas Fault is responsible for a break of slope in the earthquake size distribution. This slope increases with an increasing creep rate for larger magnitude ranges, whereas it shows no systematic dependence on creep rate for smaller magnitude ranges. This is interpreted as a deficit of large events under conditions of faster creep where seismic ruptures are less likely to propagate. These results suggest that the earthquake size distribution does not only depend on the level of stress but also on the type of deformation.

### 1. Introduction

The earthquake size distribution of seismic moment is the most widely used and best documented power law relationship in the mechanics of earthquake faulting. Using the magnitude of earthquakes instead of the seismic moment, it follows in almost all cases the well-known Gutenberg-Richter (GR) law [Gutenberg and Richter, 1944]

$$\log_{10}(N) = a - bM, \quad (1)$$

where  $N$  is the number of earthquakes with a magnitude larger than  $M$  and  $a$  and  $b$  are two positive constants. The  $a$ -value measures the productivity which depends on the space-time window of observation. The slope  $b$  is a scaling parameter which is of critical importance in seismic hazard assessment as it theoretically gives the characteristic recurrence time of large and rare events with respect to the rate of smaller and more frequent earthquakes [Wiemer and Wyss, 1997].

The typical  $b$ -value is close to 1, but values ranging from 0.3 to 2.5 have been reported in the literature [El-Isa and Eaton, 2014]. Some of these variations may be artifacts of incomplete catalogs or method of computation [Mignan and Woessner, 2012]. Nevertheless, multiple observations show significant temporal and spatial variations of  $b$ -value which have been attributed to changes in stress condition [Scholz et al., 1986; Wyss et al., 2004], loading rate [Amelung and King, 1997; Wiemer and Wyss, 1997], and structural or compositional properties [Wyss et al., 2004]. Commonly, low  $b$ -values are associated with high stress [Schorlemmer et al., 2005], low loading rate [Tormann et al., 2014], low heterogeneity [Mogi, 1962], and small fractal dimension of the seismogenic faults surface [Aki, 1981; Legrand, 2002]. However, the negative dependence on the level of stress is the strongest among the others, and it is now commonly admitted that variations in  $b$ -value can be used to assess relative changes in the level of stress [Narteau et al., 2009].

Although the GR law continues to be validated in a wide range of conditions, a number of observations suggest also that the earthquake size distribution may have significant deviation from a single power law model. For large magnitudes, characteristic earthquakes with a higher rate than predicted by the GR law have been proposed [Schwartz and Coppersmith, 1984; Wesnousky, 1994]. Such a distribution peaked at a single magnitude is not statistically confirmed, and in the vast majority of cases, the GR law cannot be rejected in favor of a characteristic earthquake model [Naylor et al., 2009]. Alternatively, a lack of large earthquakes due to a limited extent of the downdip width of the fault has been proposed [Romanovicz, 1992; Main, 2000]. At the lower end of the magnitude range, a deficit of small events was reported in the number of studies focusing on catalog completeness [Rydelek and Sacks, 1989; Taylor et al., 1990]. Along creeping faults, a deviation

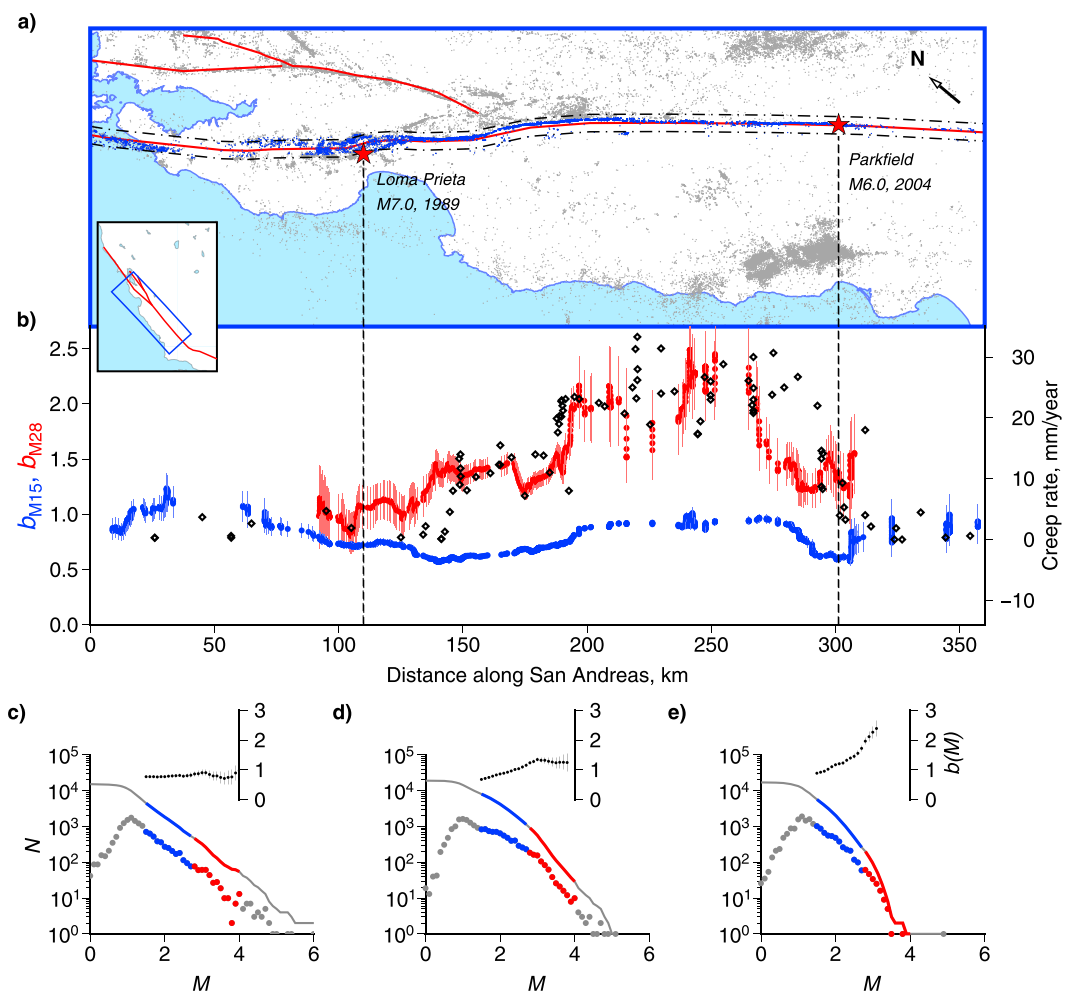


**Figure 1.** Creep rate and break of slope in earthquake size distributions along the SAF system. (a) Seismicity along the central segment of the SAF (Northern California Earthquake Data Center (NCEDC) earthquakes used in this study are shown in blue). (b) Surface creep rate measurements (black diamonds),  $b_{M1.5}$ -values (blue dots), and  $b_{M2.8}$ -values (red dots). Error bars are standard deviations obtained by bootstrap resampling. Changes in earthquake size distributions according to creep rate along the SAF system: (c) low creep rate  $<10$  mm/yr, (d) moderate creep rate from 10 to 20 mm/yr, and (e) fast creep rate  $>20$  mm/yr. The two magnitude ranges shown in Figure 1b are highlighted with the same colors. Insets show the dependence of the  $b$ -value on the lower cutoff of magnitude for overlapping magnitude ranges of width 1.2.

from scale invariant distributions has been associated with aseismic slip in the earthquake nucleation phase [Heimpel and Malin, 1998], which may result in an apparent deficit of smaller events [Tormann et al., 2014]. Here we concentrate on the dependence of the earthquake size distribution on creep rate along the San Andreas and Hayward-Calaveras fault systems. We do not consider a single power law regime; instead, we study the evolution of the  $b$ -value over two consecutive magnitude ranges to isolate the impact of fault coupling on earthquake statistics.

## 2. Creep Rate Along the San Andreas Fault System

In Northern and Central California, the Calaveras, Hayward, and San Andreas fault systems accommodate a significant fraction of the dextral motion between the North American and Pacific plates (Figures 1a and 2a). Individual faults have locked and creeping sections with well-documented creep rate [Weldon et al., 2013].

Along the San Andreas Fault (SAF), two major earthquakes ruptured the central and northern segments in 1857 and 1906, respectively. At the present time, these two segments are almost aseismic, and the entire plate interface appears to be fully locked to a depth of about 20 km. Between them lies the creeping section of the

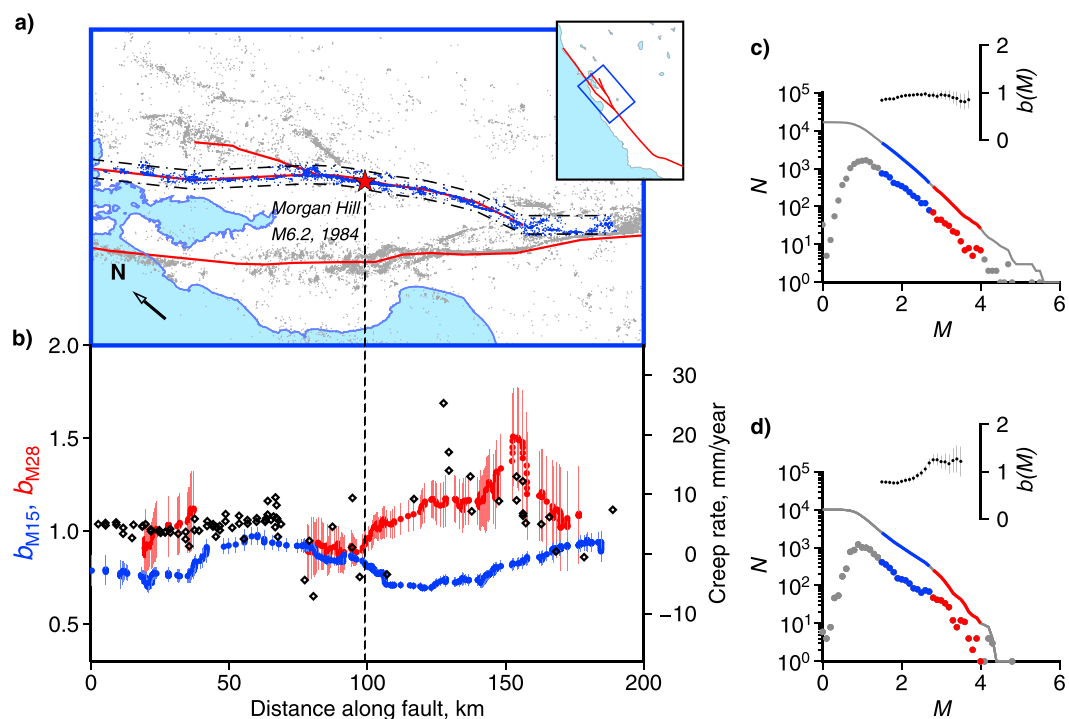


**Figure 2.** Creep rate and break of slope in earthquake size distributions along the Hayward-Calaveras fault system. (a) Seismicity along the Hayward and Calaveras faults (NCEDC earthquakes used in this study are shown in blue). (b) Surface creep rate measurements (black diamonds),  $b_{M1.5}$ -values (blue dots), and  $b_{M2.8}$ -values (red dots). Error bars are standard deviations obtained by bootstrap resampling. Changes in earthquake size distributions according to creep rate along the Hayward and Calaveras faults: (c) low creep rate  $<10$  mm/yr and (d) moderate creep rate from 10 to 20 mm/yr. The two magnitude ranges shown in Figure 2b are highlighted with the same colors. Insets show the dependence of the  $b$ -value on the lower cutoff of magnitude for overlapping magnitude ranges of width 1.2.

SAF. At its northern end, where the  $M_L$  7.0 Loma Prieta earthquake occurred in 1989 [Waldhauser and Schaff, 2008], the creep rate is close to zero (0–140 km in Figures 1a and 1b). Southward, till the junction with the Calaveras faults, the SAF exhibits a constant creep rate of  $12 \pm 2$  mm/yr (140–190 km in Figures 1a and 1b). The maximum surface creep rate of  $25 \pm 5$  mm/yr is detected in the southern part of the creeping section (190–280 km in Figures 1a and 1b). In the Parkfield section, where a  $M_w$  6.0 earthquake occurred in 2004, the creep rate decreases rapidly from 25 mm/yr to zero (280–310 km in Figures 1a and 1b).

Along the Calaveras fault, the creep rate data are more scattered. A moderate surface creep rate of  $10 \pm 3$  mm/yr is currently observed north of the junction with the SAF (120–160 km in Figures 2a and 2b). Where the  $M_L$  6.2 Morgan Hill earthquake occurred in 1984, the geodetic measurements show strong dispersion suggesting that the fault is partially locked (70–110 km in Figures 2a and 2b). Northward, the Hayward fault is creeping along all its length with a slow rate of  $5 \pm 2$  mm/yr (0–70 km in Figures 2a and 2b). This is one of the best documented examples of continuous creep along a major plate boundary.

### 3. Break of Slope in Earthquake Size Distribution and Creep Rate

In addition to these creep rates, the Northern California Earthquake Data Center (NCEDC) provides a double-difference earthquake catalog [Waldhauser and Schaff, 2008; Waldhauser, 2009], which is assumed to be complete down to  $M=1.5$  since 1984 along the studied segments of the San Andreas, Calaveras, and Hayward fault systems (supporting information). Major fault segments appear as subvertical strike-slip faults, and their recorded earthquake hypocenters can be clearly distinguished from events occurring along the surrounding seismogenic structures. According to the geometry of the surface traces of the San Andreas, Calaveras, and Hayward faults [Field et al., 2014], we select  $M \geq 1.5$  earthquakes in narrow bands of 7 km wide down to focal depths of 20 km from 1984 to 2015. Then, we classify these events according to their position along the faults using an overlapping sliding window with steps of 0.2 km and a length of 40 km. For each fault segment, we study the earthquake size distribution in two nonintersecting magnitude ranges, [1.5, 2.7] and [2.8, 4.0], using

the truncated GR law (supporting information). For both magnitude ranges, we compute the corresponding  $b$ -values,  $b_{M1.5}$  and  $b_{M2.8}$ , using maximum likelihood method for grouped data in the truncated interval of magnitude [Aki, 1965; Bender, 1983; Vorobieva *et al.*, 2013]. The  $b$ -values are assigned to the mean position of earthquakes in the current 40 km sliding window. The minimum number of events for the determination of the  $b$ -value is set to 50, but it reaches several hundreds in the [2.8, 4.0] magnitude range and several thousands in the [1.5, 2.7] magnitude range (supporting information). Thus, we analyze the spatial variation of the long-term  $b$ -values with respect to both the distance along the faults and the magnitude range. Furthermore, we compute the uncertainty of our  $b$ -value estimates by bootstrapping in order to identify those areas with significant change in slope according to sample size.

Along the SAF, the  $b_{M1.5}$ -values can be determined almost everywhere, except in two aseismic parts of the fault along the Peninsula (30–60 km in Figures 1a and 1b) and the Cholame-Carrizo (320–340 km in Figures 1a and 1b) sections. Meanwhile, the number of  $M \geq 2.8$  earthquakes allows determination of the  $b_{M2.8}$ -values from the Santa Cruz Mountain to the Parkfield sections (85–310 km in Figures 1a and 1b). Over these 200 km of active faulting, the  $b_{M2.8}$ -value varies by a factor of up to 2. It is about  $1.0 \pm 0.1$  in the Santa Cruz Mountain section (85–130 km in Figures 1a and 1b) and grows up to  $1.3 \pm 0.1$  in the northern segment of the creeping section (140–190 km in Figures 1a and 1b). Maximum values of  $2.1 \pm 0.2$  are reached along the creeping section south of the junction with the Calaveras fault (190–270 km in Figures 1a and 1b). North of the Parkfield section (280–310 km in Figures 1a and 1b), the  $b_{M2.8}$ -value drops to  $1.3 \pm 0.2$ . All together, Figure 1b shows positive correlation between the  $b_{M2.8}$ -value and the creep rate. Considering only earthquakes down to a depth of 7 km, this correlation is even more evident [Templeton *et al.*, 2008; Spada *et al.*, 2013; Murray *et al.*, 2001] (supporting information). In comparison, the  $b_{M1.5}$ -value is more stable along the SAF and shows no clear correlation with the creep rates. The  $b_{M1.5}$ -value is  $0.7 \pm 0.1$  along sections with moderate creep rates but exhibits larger values along both locked ( $1.0 \pm 0.1$ ) and fast creeping sections ( $0.9 \pm 0.1$ ).

Along the Hayward and Calaveras faults, the behaviors of the  $b_{M2.8}$ - and  $b_{M1.5}$ -values are similar to those observed along the SAF (Figure 2b). Higher creep rates are associated with larger  $b_{M2.8}$ -values, whereas there is no systematic dependence of the  $b_{M1.5}$ -value on creep rate.

Along creeping sections of the SAF and Hayward-Calaveras faults there are significant differences between the  $b_{M2.8}$  and  $b_{M1.5}$ , much larger than their uncertainties, regardless of the sample size (Figures 1b and 2b). In addition, the earthquake size distributions constructed from catalogs combining all the events occurring along locked, moderate, and fast creeping sections (Figures 1c–1e, 2c, and 2d) show the same break in the frequency-magnitude statistics with a much larger number of events ( $> 200$ ). These results suggest that in zones of moderate and high creep rates, there is not a single power law continuum extending smoothly across the entire magnitude range. Instead, there is an apparent break of slope at magnitudes around 2.8.

#### 4. Concluding Remarks

The band-limited study of  $b$ -values does not require a priori knowledge about the specific shape of the earthquake size distribution. Using two magnitude ranges, our goal is to investigate if a single power law regime can fully describe seismicity in zones of continuous deformation. Based on this initial assumption, our results show that locked seismogenic zones generally obey the GR law, whereas creep processes break it down, promoting instead band-limited scaling functions. It can take the form of breaks of slope, but other relationships could also be tested against the data.

A departure from a single power law regimes in zones of high creep rate was previously observed in California [Tormann *et al.*, 2014]. It was proposed that fast creep rates occur under low stress conditions for which microasperities start sliding aseismically. Considering the GR law derived from large events, this could explain the relative deficit of small earthquakes and the subsequent break of slope in the earthquake size distributions at lower magnitude ranges ( $M < 2.7$ ). However, this hypothesis is tantamount to assuming that within these magnitude ranges, the  $b$ -value should decrease with increasing creep rates. Our observations do not support such an hypothesis as the size distributions of  $M \in [1.5, 2.7]$  earthquakes exhibit the same scaling behavior along all the locked and creeping sections of the San Andreas, Hayward, and Calaveras faults (blue symbols in Figure 3). On the opposite, the scaling behavior of  $M \in [2.8, 4]$  earthquakes varies significantly and shows the same positive correlation with creep rate along all the different faults (red symbols in Figure 3). We conclude that creeping and locked segments obey the same scaling law over lower magnitude ranges but

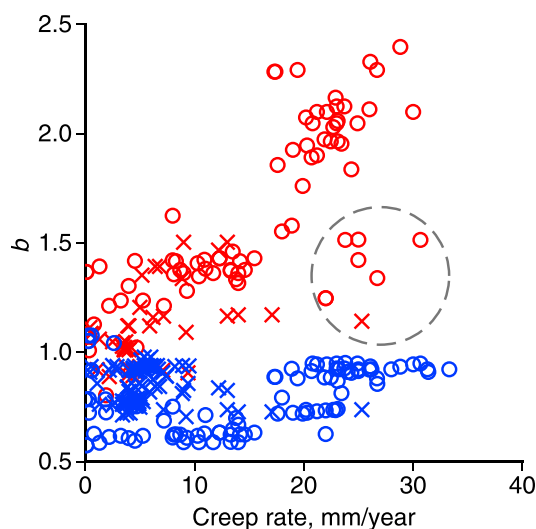


**Figure 3.** Dependence of the slope of earthquake size distribution on creep rate. The  $b$ -values in two consecutive magnitude ranges, [1.5, 2.7] (blue) and [2.8, 4.0] (red), along the SAF (circles) and the Hayward-Calaveras faults (crosses). The dashed circle contains six points from the transition zone between fast creeping and locked segments in the south of San Andreas (supporting information) and one point from Calaveras where there is a single creep measurement strongly exceeding other measurements in this area.

suggest that the integrated response along the SAF and Hayward-Calaveras faults is a break of slope in the earthquake size distribution and its positive dependency on creep rate.

In addition to scaling exponents, limits of power law regimes can provide useful insight in earthquake physics. Here we show that breaks of slope in earthquake size distributions occur for magnitudes between 2.5 and 3.0. Such a characteristic magnitude is independent of creep rate (Figures 1d, 1e, and 2d) and may be translated into a characteristic length scale of 300 m using classical empirical formula [Wells and Coppersmith, 1994]. Such a length scale is more than 1 order of magnitude smaller than the seismogenic thickness ( $\approx 10$  km), but on the order of the width of the fault zone damage, where low internal friction, fluid-rock coupling, and viscous processes may prevent the full range of elastic interactions and then modify the scaling behavior of larger earthquakes. In the western Alps, Sue *et al.* [2002] document the same type of earthquake size distributions with or without breakdown for largest events and use a numerical model for reproducing these differences depending on the internal friction angle. Such a model and our observations are compatible with results of laboratory experiments that show that rock samples of the creeping section of the San Andreas Fault are extremely weak (a friction coefficient  $\mu \approx 0.1$ ) and exhibit both velocity strengthening frictional behavior and anomalously low rates of frictional healing [Carpenter *et al.*, 2012]. Furthermore, different deformation regimes caused by changes in material properties with depth, including brittle-ductile transition, may affect the earthquake size distributions [Mori and Abercrombie, 1997; Amitrano, 2003; Amorèse *et al.*, 2010].

Our study on a major continental transform fault shows that in addition to the level of stress, earthquake size distributions can be used to infer plate coupling and zones of more continuous deformation. This may be particularly important along subduction zones where various types of slow earthquakes [Ide *et al.*, 2007; Villegas-Lanza *et al.*, 2016] and changes in  $b$ -values are increasingly reported [Nishikawa and Ide, 2014]. In such places, which exhibit more than a single power law regime, the identification of break of slopes in the earthquake size distributions may also contribute to better assessment of earthquake hazards.

### References

Aki, K. (1965), Maximum likelihood estimate of  $b$  in the formula  $\log N = a - bM$  and its confidence level, *Bull. Earthquake Res. Inst.*, *43*, 237–239.  
 Aki, K. (1981), A probabilistic synthesis of precursory phenomena, in *Earthquake Prediction. An International Review* Maurice Ewing Ser., edited by D. Simpson and P. Richards, pp. 566–574, AGU, Washington, D. C.

that there is a deficit of large events along creeping segments as seismic ruptures are less likely to propagate in zone of continuous deformation.

The intrinsic scale invariance for earthquake sizes as expressed by the GR law is thought to result from structural and compositional heterogeneities combined with a variety of interacting physical/chemical processes [Ben-Zion, 2008]. Nevertheless, using the diversity of slip behaviors identified along active fault zones (e.g., tremor, low-frequency earthquakes, slow slip events, and silent earthquakes), it was shown that these events exhibit different scaling and spectral properties [Ide *et al.*, 2007] than earthquakes. As these two different expressions of along-fault deformation are likely to interact with one another, it is not surprising to observe changes in earthquake size distribution in zones where various slip behaviors coexist [Wei *et al.*, 2013]. Moreover, creep accommodates a significant amount of deformation at large length and time scales, so that it is efficient in increasing the number of small magnitude events and at modulating large-scale seismic activity. Our results

### Acknowledgments

We acknowledge financial support of C.N. from the UnivEarthS LabEx program of Sorbonne Paris Cité (ANR-10-LABX-0023 and ANR-11-IDEX-0005-02) and the French National Research Agency (ANR-12-BS05-001-03/EXO-DUNES) and of P.S. from the Russian Science Foundation, Project 15-17-00093. Authors are grateful to R. Scherbakov and to an anonymous reviewer for helping to improve the manuscript. The data used are listed in the references.

- Amelung, F., and G. King (1997), Earthquake scaling laws for creeping and non-creeping faults, *Geophys. Res. Lett.*, *24*, 507–510, doi:10.1029/97GL00287.
- Amitrano, D. (2003), Brittle-ductile transition and associated seismicity: Experimental and numerical studies and relationship with the  $b$  value, *J. Geophys. Res.*, *108*(B1), 2044, doi:10.1029/2001JB000680.
- Amorèse, D., J. Grasso, and P. Rydelek (2010), On varying  $b$ -values with depth: Results from computer-intensive tests for Southern California, *Geophys. J. Int.*, *180*(1), 347–630, doi:10.1111/j.1365-246X.2009.04414.x.
- Ben-Zion, Y. (2008), Collective behavior of earthquakes and faults: Continuum-discrete transitions, progressive evolutionary changes and different dynamic regimes, *Rev. Geophys.*, *46*, RG4006, doi:10.1029/2008RG00026.
- Bender, B. (1983), Maximum likelihood estimation of  $b$ -values for magnitude grouped data, *Bull. Seismol. Soc. Am.*, *73*, 831–851.
- Carpenter, B. M., D. M. Saffer, and C. Marone (2012), Frictional properties and sliding stability of the San Andreas Fault from deep drill core, *Geology*, *40*, 759–762, doi:10.1130/G33007.1.
- El-Isa, Z., and D. W. Eaton (2014), Spatiotemporal variations in the  $b$ -value of earthquake magnitude-frequency distributions: Classification and causes, *Tectonophysics*, *615*, 1–11.
- Field, E. H., et al. (2014), Uniform California earthquake rupture forecast, version 3 (UCERF3)—The time-independent model, *Bull. Seismol. Soc. Am.*, *104*(3), 1122–1180, doi:10.1785/0120130164.
- Gutenberg, B., and C. F. Richter (1944), Frequency of earthquakes in California, *Bull. Seismol. Soc. Am.*, *34*, 185–188.
- Heimpel, M., and P. Malin (1998), Aseismic slip in earthquake nucleation and self-similarity: Evidence from Parkfield, California, *Earth Planet. Sci. Lett.*, *157*, 249–254.
- Ide, S., G. C. Beroza, D. R. Shelly, and T. Uchide (2007), A scaling law for slow earthquakes, *Nature*, *447*(7140), 76–79.
- Legrand, D. (2002), Fractal dimensions of small, intermediate, and large earthquakes, *Bull. Seismol. Soc. Am.*, *92*, 3318–3320.
- Main, I. (2000), Apparent breaks in scaling in the earthquake cumulative frequency-magnitude distribution: Fact or artifact?, *Bull. Seismol. Soc. Am.*, *90*, 86–97.
- Mignan, A., and J. Woessner (2012), Estimating the magnitude of completeness for earthquake catalogs, *Commun. Online Resour. Stat. Seismic. Anal.*, *45*, doi:10.5078/corssa-00180805.
- Mogi, K. (1962), Magnitude-frequency relationship for elastic shocks accompanying fractures of various materials and some related problems in earthquakes, *Bull. Earthquake Res.*, *40*, 831–883.
- Mori, J., and R. E. Abercrombie (1997), Depth dependence of earthquake frequency-magnitude distributions in California: Implication for rupture initiation, *J. Geophys. Res.*, *102*(B7), 15,081–15,090.
- Murray, J., P. Segall, and P. Cervelli (2001), Inversion of GPS data for spatially variable slip-rate on the San Andreas Fault near Parkfield, *Geophys. Res. Lett.*, *28*, 359–362, doi:10.1029/2000GL011933.
- Narteau, C., S. Byrdina, P. Shebalin, and D. Schorlemmer (2009), Common dependence on stress for the two fundamental laws of statistical seismology, *Nature*, *462*, 642–645, doi:10.1038/nature08553.
- Naylor, M., J. Greenhough, J. McCloskey, A. Bell, and I. Main (2009), Statistical evaluation of characteristic earthquakes in the frequency-magnitude distributions of Sumatra and other subduction zone regions, *Geophys. Res. Lett.*, *36*, 249–254, doi:10.1029/2009GL040460.
- Nishikawa, T., and S. Ide (2014), Earthquake size distribution in subduction zones linked to slab buoyancy, *Nat. Geosci.*, *7*(12), 904–908.
- Romanoviz, B. (1992), Strike-slip earthquakes on quasi-vertical transcurrent faults: Inferences for general scaling relations, *Geophys. Res. Lett.*, *19*, 481–484, doi:10.1029/92GL00265.
- Rydelek, P. A., and I. S. Sacks (1989), Testing the completeness of earthquake catalogs and the hypothesis of self-similarity, *Nature*, *337*, 251–253.
- Scholz, C., C. Aviles, and S. Wesnousky (1986), Scaling differences between large intraplate and interplate earthquakes, *Bull. Seismol. Soc. Am.*, *76*, 65–70.
- Schorlemmer, D., S. Wiemer, and M. Wyss (2005), Variations in earthquake-size distribution across different stress regimes, *Nature*, *437*, 539–542.
- Schwartz, D., and K. Coppersmith (1984), Fault behavior and characteristic earthquake: Examples from the Wasatch and San Andreas Fault zones, *J. Geophys. Res.*, *89*(B7), 5681–5698.
- Sue, C., J. R. Grasso, F. Lahaie, and D. Amitrano (2002), Mechanical behavior of western alpine structures inferred from statistical analysis of seismicity, *Geophys. Res. Lett.*, *29*(8), 1224, doi:10.1029/2001GL014050.
- Spada, M., T. Tormann, S. Wiemer, and B. Enescu (2013), Generic dependence of the frequency-size distribution of earthquakes on depth and its relation to the strength profile of the crust, *Geophys. Res. Lett.*, *40*, 709–714, doi:10.1029/2012GL054198.
- Taylor, D. W. A., J. A. Snoke, I. S. Sacks, and T. Takanami (1990), Nonlinear frequency-magnitude relationships for the Hokkaido Corner, Japan, *Bull. Seismol. Soc. Am.*, *80*, 340–353.
- Templeton, D., R. Nadeau, and R. Burgmann (2008), Behavior of repeating earthquake sequences in Central California and implications for subsurface fault creep, *Bull. Seismol. Soc. Am.*, *98*(1), 52–65, doi:10.1785/0120070026.
- Tormann, T., S. Wiemer, and A. Mignan (2014), Systematic survey of high-resolution  $b$  value imaging along californian faults: Inference on asperities, *J. Geophys. Res. Solid Earth*, *119*, 2029–2054, doi:10.1002/2013JB010867.
- Villegas-Lanza, J., J.-M. Nocquet, F. Rolandone, M. Vallée, H. Tavera, F. Bondoux, T. Tran, X. Martin, and M. Chlieh (2016), A mixed seismic-aseismic stress release episode in the Andean subduction zone, *Nat. Geosci.*, *9*, 150–154, doi:10.1038/ngeo2620.
- Vorobieva, I., C. Narteau, P. Shebalin, F. Beaucaud, A. Nercessian, V. Clourad, and M.-P. Bouin (2013), Multiscale mapping of completeness magnitude of earthquake catalogs, *Bull. Seismol. Soc. Am.*, *103*, 2188–2202, doi:10.1785/0120120132.
- Waldhauser, F. (2009), Near-real-time double-difference event location using long-term seismic archives, with application to Northern California, *Bull. Seismol. Soc. Am.*, *99*, 2736–2848, doi:10.1785/0120080294.
- Waldhauser, F., and D. Schaff (2008), Large-scale relocation of two decades of Northern California seismicity using cross-correlation and double-difference methods, *J. Geophys. Res.*, *113*, B08311, doi:10.1029/2007JB005479.
- Wei, M., Y. Kaneko, Y. Liu, and J. J. McGuire (2013), Episodic fault creep events in California controlled by shallow frictional heterogeneity, *Nat. Geosci.*, *6*(7), 566–570.
- Weldon, R. J., II, D. A. Schmidt, J. L. Austin, E. M. Weldon, and T. E. Dawson (2013), Appendix D: Compilation of creep rate data for California faults and calculation of moment reduction due to creep, in Uniform California earthquake rupture forecast, version 3 (UCERF3)—The time-independent model, U.S. Geol. Surv. Open-File Rep. 2013–1165, U.S. Geol. Surv., Denver, Colo. [Available at [http://pubs.usgs.gov/of/2013/1165/pdf/ofr2013-1165\\_appendixD.pdf](http://pubs.usgs.gov/of/2013/1165/pdf/ofr2013-1165_appendixD.pdf), accessed 13.02.2014.]
- Wells, D., and K. Coppersmith (1994), New empirical relationships among magnitude, rupture length, rupture width, rupture area, and surface displacement, *Bull. Seismol. Soc. Am.*, *84*, 974–1002.
- Wesnousky, S. (1994), The Gutenberg-Richter or characteristic earthquake distribution, which is it?, *Bull. Seismol. Soc. Am.*, *84*(6), 1940–1959.

Wiemer, S., and M. Wyss (1997), Mapping the frequency-magnitude distribution in asperities: An improved technique to calculate recurrence times?, *J. Geophys. Res.*, *102*, 15,115–15,128, doi:10.1029/97JB00726.

Wyss, M., C. Sammis, R. Nadeau, and S. Wiemer (2004), Fractal dimension and *b*-value on creeping and locked patches of the San Andreas Fault near Parkfield, California, *Bull. Seismol. Soc. Am.*, *94*, 410–421.